

Character of the phase transitions in the Haldane-Hubbard model with ionic potentials

Hao Yuan,¹ Yangbin Guo,¹ Ruifeng Lu,¹ Hantao Lu,² and Can Shao^{1,*}

¹*Institute of Ultrafast Optical Physics, Department of Applied Physics, Nanjing University of Science and Technology, Nanjing 210094, China*

²*School of Physical Science and Technology & Key Laboratory for Magnetism and Magnetic Materials of the MoE, Lanzhou University, Lanzhou 730000, China*

Using the exact-diagonalization approach, we revisit the ground-state phase diagram of the Haldane-Hubbard model on the honeycomb lattice with staggered sublattice potentials. The phase diagram includes the band insulator, Mott insulator and two Chern insulator phases with Chern numbers $C = 2$ and $C = 1$. The character of transitions between different phases is studied by analyzing the lower-lying energy levels, excitation gaps, structure factors and fidelity metric. We find that the $C = 1$ phase with one of the spin components in Hall state and the other one in localized state, can be continuously deformed into the $C = 2$ phase without a gap closure, while all the other phase transitions are found to be first-order ones as expected. Our finding may enrich the understanding of topological phase transitions in condensed-matter physics.

Introduction.— As one of the most important concept in condensed matter physics, the Landau-Ginzburg theory describes the phase transitions of matter that are caused by the spontaneous breaking of certain symmetries [1]. While the discovery of the integer quantum Hall effect in a two-dimensional electron gas under strong magnetic field provided another paradigm to characterize quantum states [2]. In the past few decades, the topological aspects have played an increasingly important role as a new standard for the classification of a large class of materials [3–6], and the topological ordered states in non-interaction systems have been completely classified based on time-reversal, particle-hole, chiral and crystal symmetries [7–10].

In the interacting systems, the correlation effect of electrons is expected to give rise to more intriguing and richer phenomena [11]. A famous example is the fractional quantum Hall state, which allows the emergence of quasiparticle excitations that carry fractional charge and obey fractional statistics largely due to the strong repulsion among electrons [12–14]. On the other hand, the electronic interactions may directly lead to the so-called topological Mott insulator via a dynamically generated spin-orbit coupling [15–23]. Despite the fact that some of these mean-field results remain controversial [24–28], interaction-induced topological states may still be observed in two-dimensional systems with quadratic band crossing and weak interactions [29–36]. Finally, the interplay between topology and local orders has been largely addressed by introducing interaction to topological systems [37–43]. For example, an exotic phase with one of the spin components in the Hall state and the other one in a localized state can emerge in the spinful Haldane-Hubbard model with inversion-breaking ionic potentials [39–42].

In this Letter, we adopt the exact-diagonalization (ED) method to study the spinful Haldane-Hubbard model at half-filling and zero temperature. By tuning the strength

parameters of the staggered sublattice potential Δ and the on-site Coulomb interaction U , we explore its ground-state phase diagram. Our results are similar to those obtained by Vanhala et al. [39], and the intermediate phases with the Chern number $C = 1$ can be also observed. Other phases include the band insulator, Mott insulator and topological insulator with $C = 2$. Here, we aim to identify the nature of phase transitions by analyzing the excitation gaps, structure factors and fidelity metrics in ED results, which gives unbiased information in finite-size systems. In non-interacting systems, the transition between distinct topological phases usually involves a bulk band gap closing at the critical point and across it the Chern number changes [44, 45]. While in our case, a continuous phase transition without gap closing appears between the two topological phases with $C = 1$ and $C = 2$, and all the other phase transitions are found to be first-order ones as usual.

Model and measurements— We write the Hamiltonian of the Haldane-Hubbard model as $\hat{H} = \hat{H}_k + \hat{H}_l$, where the kinetic part

$$\begin{aligned} \hat{H}_k = & -t_1 \sum_{\langle i,j \rangle, \sigma} (\hat{c}_{i,\sigma}^\dagger \hat{c}_{j,\sigma} + \text{H.c.}) \\ & -t_2 \sum_{\langle\langle i,j \rangle\rangle, \sigma} (e^{i\phi_{ij}} \hat{c}_{i,\sigma}^\dagger \hat{c}_{j,\sigma} + \text{H.c.}) \end{aligned} \quad (1)$$

and the local part

$$\hat{H}_l = -U \sum_i \hat{n}_{i,\uparrow} \hat{n}_{i,\downarrow} + \Delta \sum_{i,\sigma} \text{sgn}(i) \hat{n}_{i,\sigma}. \quad (2)$$

Here, $\hat{c}_{i,\sigma}^\dagger$ ($\hat{c}_{i,\sigma}$) creates (annihilates) an electron at site i of the honeycomb lattice with spin $\sigma = \uparrow$ or \downarrow , and $\hat{n}_{i,\sigma} \equiv \hat{c}_{i,\sigma}^\dagger \hat{c}_{i,\sigma}$ is the number operator. t_1 (t_2) is the nearest-neighbor (next-nearest-neighbor) hopping constant; U is the on-site interaction strength; Δ is the staggered potential. $\text{sgn}(i)$ equals $+1$ for sublattice A and -1

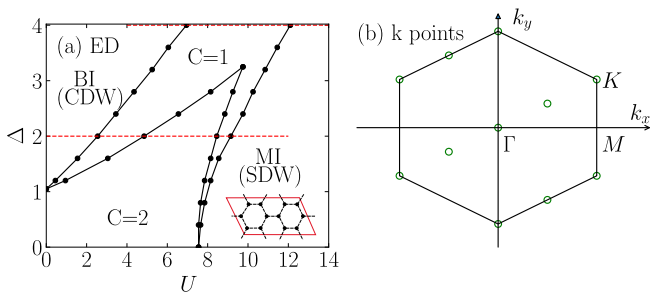


FIG. 1. (a) Phase diagram in the parametric space (U, Δ) of the Haldane-Hubbard model based on the exact diagonalization approaches. The black solid lines indicate the phase boundaries where the Chern number changes. The red dashed lines denote the parameters we choose to show more details below. The inset on the bottom left depicts the 12A cluster with periodic boundary condition. (b) The set of k points in the first Brillouin zone for the 12A cluster along with the high-symmetry points Γ , M , and K .

for sublattice B, respectively. The phase $\phi_{i,j} = \phi (-\phi)$ in the clockwise (anticlockwise) loop is introduced to the second hopping term. Throughout the paper, we focus on the ground-state phase diagram at half-filling.

Several properties can be used to characterize the quantum phase transition. One of them is the ground-state fidelity metric, which is defined as [46–48] :

$$g(U, \delta U) \equiv \frac{2}{N} \frac{1 - |\langle \Psi_0(U) | \Psi_0(U + \delta U) \rangle|}{(\delta U)^2}, \quad (3)$$

with $|\psi_0(U)\rangle$ [$|\psi_0(U + \delta U)\rangle$] being the ground state of $\hat{H}(U)$ [$\hat{H}(U + \delta U)$]. In what follows, we set $\delta U = 10^{-3}$. In finite-size systems, this quantity is expected to exhibit a large and sharp peak or discontinuity for the first-order transition, while there is a wider and smaller “hump” for the continuous transition [38, 49, 50].

The spin-density wave (SDW) and charge-density wave (CDW) structure factors can be used to characterize the Mott insulator (MI) and band insulator (BI), respectively. We define them in a staggered fashion as follows:

$$S_{\text{SDW}} = \frac{1}{N} \sum_{i,j} (-1)^\eta \langle (\hat{n}_{i,\uparrow} - \hat{n}_{i,\downarrow})(\hat{n}_{j,\uparrow} - \hat{n}_{j,\downarrow}) \rangle,$$

$$S_{\text{CDW}} = \frac{1}{N} \sum_{i,j} (-1)^\eta \langle (\hat{n}_{i,\uparrow} + \hat{n}_{i,\downarrow})(\hat{n}_{j,\uparrow} + \hat{n}_{j,\downarrow}) \rangle, \quad (4)$$

where $\eta = 0$ ($\eta = 1$) indicates that sites i and j are in the same (different) sublattice.

The topological invariant is quantified by the Chern number. Given the twisted boundary conditions (TBCs) [51], it can be defined as [52],

$$C = \int \frac{d\phi_x d\phi_y}{2\pi i} \langle (\partial_{\phi_x} \Psi^* | \partial_{\phi_y} \Psi) - (\partial_{\phi_y} \Psi^* | \partial_{\phi_x} \Psi) \rangle, \quad (5)$$

where $|\Psi\rangle$ is the ground-state wave function, and ϕ_x (ϕ_y) is the twisted phase along the x (y) direction. To

avoid the integration with huge computational resources needed, we instead use a sufficiently discretized version that is able to converge to the result of Eq. (5) [37, 53, 54]. Here, a mesh of 6×6 phases (ϕ_x, ϕ_y) is sufficiently enough to guarantee the convergence.

In what follows, t_1 is set to be the unit of energy and $t_2 = 0.2$. We further fix the Haldane phase ϕ to $\pi/2$, in order to maximize the Chern insulating (CI) phase [49, 55].

Results and analysis— By employing the Arnoldi [56] method, we can obtain the ground state and several excited states of the Haldane-Hubbard model. We choose the 12A cluster with periodic boundary condition (PBC), shown in the bottom right corner of Fig. 1 (a). It has been noticed that compared to other 12-, 16- and 18-site lattices, this cluster, whose reciprocal lattice contains the Γ point, all the K points and one pair of M points [see Fig. 1 (b)], is more suitable for the purpose of ED analysis in the interacting Haldane model [38]. Clusters with better symmetries than 12A need at least 24 sites, which is unreachable for the current ED approaches.

The phase diagram in the parametric space (U, Δ) is displayed in Fig. 1(a), which is similar to that in Ref. [39]: the CI phase with $C = 2$ in the small U and Δ region; the BI (CDW) and MI (SDW) states are governed by large Δ and U , respectively; and another topological phase with $C = 1$ is sandwiched between the BI and MI phases. Different from the previous studies focusing on the phase diagram of this model, we are mainly concerned with the nature of these phase transitions. Here we choose $\Delta = 2.0$ and $\Delta = 4.0$ [red dashed lines in Fig. 1(a)] to calculate the energy levels E_α , excitation gaps $\Delta_{\text{ex}}^{(\alpha)}$, structure factors $S_{\text{SDW/CDW}}$ and fidelity metric g , as shown in Fig. 2. The first four lowest-lying energy levels are denoted E_α with $\alpha = 0, 1, 2, 3$, (E_0 is the ground-state energy) and $\Delta_{\text{ex}}^{(\alpha)} = E_\alpha - E_0$. The line of $\Delta = 2.0$ successively crosses the BI, $C = 1$, $C = 2$, $C = 1$ and MI phases with increasing U from 0.0 to 12.0, while the line of $\Delta = 4.0$ crosses the BI, $C = 2$ and MI phases as U increases from 4.0 to 14.0. Note that the phase diagram is characterized by the results of Chern number [see green dashed lines in Figs. 2(c) and 2(g) for example]. For the phase boundaries of the BI and MI phases ($U = 2.5$ and $U = 9.2$ for $\Delta = 2$; $U = 6.9$ and $U = 12.2$ for $\Delta = 4$), we can observe the characteristics of first-order phase transition close to the critical points, which includes level crossings between the ground state and one excited state in Figs. 2(a) and 2(e), excitation gaps vanishing in Figs. 2(b) and 2(f), discontinuities of the CDW and SDW structure factors in Figs. 1(c) and 2(g), as well as sharp peaks in the fidelity metrics g in Figs. 2(d) and 2(h). These features can be compared with the ED results in Ref. [39], where a gap closure was not able to be identified due to the absence of K point in their 16-site lattice.

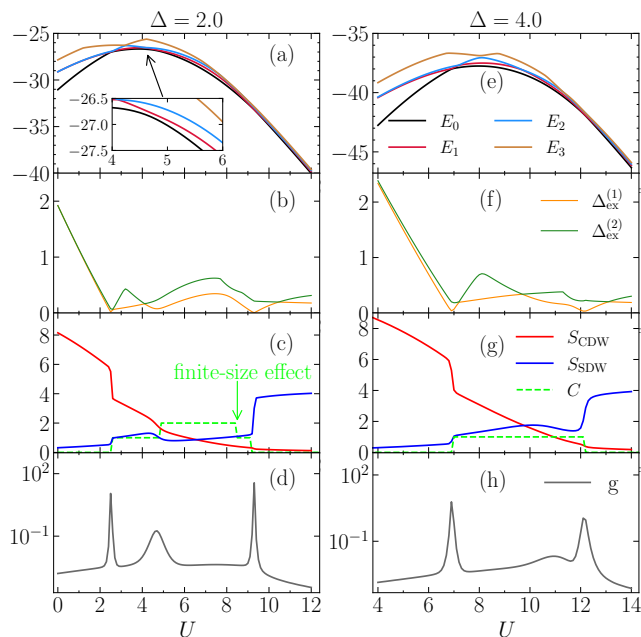


FIG. 2. (a)(e) Four lowest-lying energy levels E_α , (b)(f) the excitation gaps $\Delta_{\text{ex}}^{(\alpha)}$, (c)(g) the structure factors $S_{\text{SDW/CDW}}$ and Chern number C , and (d)(h) the fidelity metric g of the Haldane-Hubbard model with $\Delta = 2.0$ on the left panels and $\Delta = 4.0$ on the right panels. The inset in (a) shows a closeup view of the level approaching around $U = 4.8$.

Nevertheless, some features of the continuous phase transition appear at $(U, \Delta) = (4.8, 2.0)$ between the $C = 1$ and $C = 2$ phases. Rather than the aforementioned level crossing, the two lowest energy levels just approach to each other at this point, see more details in the inset of Fig. 2(a). At the same place, the decreasing of the first excitation gap $\Delta_{\text{ex}}^{(1)}$ occurs instead of gap vanishing, see Fig. 2(b). The slowly changing of structure factors and a smaller “hump” in fidelity metric can be also observed in Figs. 2(c) and 2(d), respectively. As far as we know, all phase transitions between topologically and locally ordered states in interacting Haldane systems are found to be first-order ones with gap closing at the K point [37, 50, 57]. Surprisingly, our results indicate that there is a continuous transition without gap closure between the $C = 1$ and $C = 2$ phases.

To further eliminate the finite-size effect and the possibility of the excitation gap vanishing at other k points, we adopt a mesh of 10×10 twisted phases (ϕ_x, ϕ_y) , including one PBC and 99 TBCs, to obtain their excitation gaps along the line of $\Delta = 2.0$, as shown in Fig. 3(a). Note that there are 6 k -points in the first Brillouin zone for the PBC, while there will be 600 k -points when including the additional 99 twisted phases. We find that there is no gap closure around $U = 4.8$ for either PBC or TBCs. In fact, we can not even observe the decreasing of the gap for all TBCs. Meanwhile, the changing of the

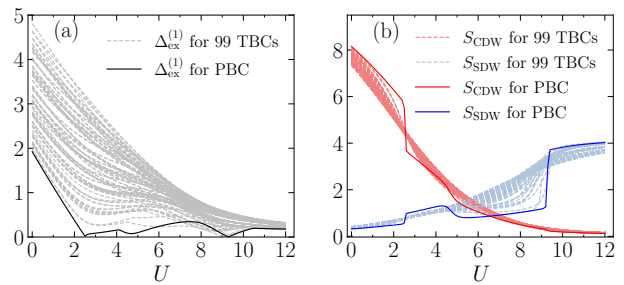


FIG. 3. (a) The excitation gaps $\Delta_{\text{ex}}^{(1)}$ and (b) the structure factors of SDW and CDW with $\Delta = 2.0$ as a function of U . Solid and dashed lines denote the results from the periodic boundary condition and 99 twisted boundary conditions, respectively.

structure factors in TBCs are much smoother than those in PBC, as shown in Fig. 3(b). Besides, for the other two first-order transition points, the TBCs are not able to grasp the fundamental critical features owing to the absence of K point.

However, for the critical point locating at $U = 8.5$ and $\Delta = 2.0$ [see green arrow in Fig. 2(c)], we do not have any other evidence about the character of transition except for the changing of Chern number. We thus speculate this narrow region, i.e., the $C = 1$ phase between the $C = 2$ and MI phase, to be a result of finite-size effect. To further verify our idea, we show the contour plots of S_{SDW} , S_{CDW} , g and $\Delta_{\text{ex}}^{(1)}$ as a function of U and Δ in Figs. 4(a), 4(b), 4(c) and 4(d), respectively. We find that except for this region, all the other phase boundaries identified by the Chern number have a very good correspondence with the results of structure factor, fidelity metric and the first excitation gap. This disagreement has also been observed in Refs. [37, 38, 50] and attributed to the finite-size effect.

Summary and Discussion— To summarize, we studied the spinful Haldane-Hubbard model at half-filling on the honeycomb lattice by the ED method. By tuning the on-site interaction strength U and staggered sublattice potential Δ , the ground state exhibits a rich phase diagram, which includes the BI (CDW) and MI (SDW) phases with local order parameters, as well as two topologically nontrivial phases with Chern number $C = 2$ and $C = 1$. We observed the energy-level crossings, the discontinuities of structure factors and the sharp peaks of fidelity metric at both BI and MI phase boundaries, signaling a first-order phase transition. However, a continuous transition with nonvanishing gap, slowly changing of structure factors and a small “hump” of fidelity metric, can be found between the two topological phases.

It is well known that the total Chern number in non-interacting systems is a summation over all occupied bands, while in the spinful interacting Haldane models, the Chern number can be regarded as the summation of the contribution from the two spin components. The

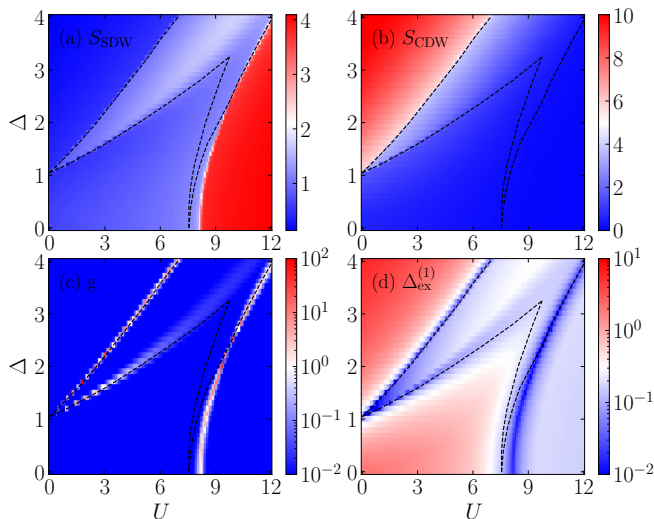


FIG. 4. Contour plots of (a) the SDW structure factor S_{SDW} , (b) the CDW structure factor S_{CDW} , (c) the fidelity metric g and (d) the first excitation gap $\Delta_{\text{ex}}^{(1)}$ as a function of U and Δ . The black dashed line denotes where the Chern numbers changes. The results are obtained from the ED method.

$C = 1$ state may indicate a spontaneous breaking of the $\text{SU}(2)$ spin-rotation symmetry [39]. With the increase of the on-site interaction U , the induced Hartree potential from one component can recover the band inversion of another component from the influence of the staggered potential Δ , driving it into a Hall state. Interestingly, for not too strong Δ , e.g., along the $\Delta = 2.0$ line, the competition between the on-site U and the staggered potential Δ can further release the remaining component into a topologically nontrivial state. The details of the mechanism of the transition, which we have argued to be a continuous one, remain to be resolved.

C. S. acknowledges support from the National Natural Science Foundation of China (NSFC; Grant No.12104229). R. F. acknowledges supports from NSFC (Grants No. 11974185) and the Natural Science Foundation of Jiangsu Province (Grant No. BK20170032). H. L. acknowledges support from NSFC (Grants No. 11874187, No. 12174168 and No. 12047501).

* shaocan@njust.edu.cn

[1] L. D. Landau and E. M. Lifshitz, *Statistical Physics, Part 1*. Vol. 5 (3rd edition) Butterworth-Heinemann, Oxford, 1980.
 [2] K. v. Klitzing, G. Dorda, and M. Pepper, *Phys. Rev. Lett.* **45**, 494 (1980).
 [3] T. Zhang, Y. Jiang, Z. Song, H. Huang, Y. He, Z. Fang, H. Weng, and C. Fang, *Nature* **566**, 475 (2019).
 [4] M. G. Vergniory, L. Elcoro, C. Felser, N. Regnault, B. A. Bernevig, and Z. Wang, *Nature* **566**, 480 (2019).

[5] F. Tang, H. C. Po, A. Vishwanath, and X. Wan, *Nature* **566**, 486 (2019).
 [6] J. Kruthoff, J. de Boer, J. van Wezel, C. L. Kane, and R.-J. Slager, *Phys. Rev. X* **7**, 041069 (2017).
 [7] A. P. Schnyder, S. Ryu, A. Furusaki, and A. W. W. Ludwig, *Phys. Rev. B* **78**, 195125 (2008).
 [8] A. Kitaev, *AIP Conference Proceedings* **1134**, 22 (2009).
 [9] J. C. Budich and B. Trauzettel, *Phys. Status Solidi RRL* **7**, 109 (2013).
 [10] R.-J. Slager, A. Mesaros, V. Juričić, and J. Zaanen, *Nat. Phys.* **9**, 98 (2013).
 [11] M. Hohenadler, T. C. Lang, and F. F. Assaad, *Phys. Rev. Lett.* **106**, 100403 (2011).
 [12] R. B. Laughlin, *Phys. Rev. Lett.* **50**, 1395 (1983).
 [13] H. L. Stormer, D. C. Tsui, and A. C. Gossard, *Rev. Mod. Phys.* **71**, S298 (1999).
 [14] C. Nayak, S. H. Simon, A. Stern, M. Freedman, and S. Das Sarma, *Rev. Mod. Phys.* **80**, 1083 (2008).
 [15] S. Raghu, X.-L. Qi, C. Honerkamp, and S.-C. Zhang, *Phys. Rev. Lett.* **100**, 156401 (2008).
 [16] J. Wen, A. Rüegg, C.-C. J. Wang, and G. A. Fiete, *Phys. Rev. B* **82**, 075125 (2010).
 [17] J. C. Budich, R. Thomale, G. Li, M. Laubach, and S.-C. Zhang, *Phys. Rev. B* **86**, 201407(R) (2012).
 [18] A. Dauphin, M. Müller, and M. A. Martin-Delgado, *Phys. Rev. A* **86**, 053618 (2012).
 [19] C. Weeks and M. Franz, *Phys. Rev. B* **81**, 085105 (2010).
 [20] A. Rüegg and G. A. Fiete, *Phys. Rev. B* **84**, 201103(R) (2011).
 [21] K.-Y. Yang, W. Zhu, D. Xiao, S. Okamoto, Z. Wang, and Y. Ran, *Phys. Rev. B* **84**, 201104(R) (2011).
 [22] T. Yoshida, R. Peters, S. Fujimoto, and N. Kawakami, *Phys. Rev. Lett.* **112**, 196404 (2014).
 [23] L. Wang, X. Dai, and X. C. Xie, *EPL (Europhysics Letters)* **98**, 57001 (2012).
 [24] N. A. García-Martínez, A. G. Grushin, T. Neupert, B. Valenzuela, and E. V. Castro, *Phys. Rev. B* **88**, 245123 (2013).
 [25] M. Daghofer and M. Hohenadler, *Phys. Rev. B* **89**, 035103 (2014).
 [26] J. Motruk, A. G. Grushin, F. de Juan, and F. Pollmann, *Phys. Rev. B* **92**, 085147 (2015).
 [27] S. Capponi and A. M. Läuchli, *Phys. Rev. B* **92**, 085146 (2015).
 [28] D. D. Scherer, M. M. Scherer, and C. Honerkamp, *Phys. Rev. B* **92**, 155137 (2015).
 [29] K. Sun, H. Yao, E. Fradkin, and S. A. Kivelson, *Phys. Rev. Lett.* **103**, 046811 (2009).
 [30] J. M. Murray and O. Vafek, *Phys. Rev. B* **89**, 201110(R) (2014).
 [31] J. W. F. Venderbos, M. Manzardo, D. V. Efremov, J. van den Brink, and C. Ortix, *Phys. Rev. B* **93**, 045428 (2016).
 [32] H.-Q. Wu, Y.-Y. He, C. Fang, Z. Y. Meng, and Z.-Y. Lu, *Phys. Rev. Lett.* **117**, 066403 (2016).
 [33] W. Zhu, S.-S. Gong, T.-S. Zeng, L. Fu, and D. N. Sheng, *Phys. Rev. Lett.* **117**, 096402 (2016).
 [34] O. Vafek and K. Yang, *Phys. Rev. B* **81**, 041401(R) (2010).
 [35] J. Wang, C. Ortix, J. van den Brink, and D. V. Efremov, *Phys. Rev. B* **96**, 201104(R) (2017).
 [36] S. Uebelacker and C. Honerkamp, *Phys. Rev. B* **84**, 205122 (2011).
 [37] C. N. Varney, K. Sun, M. Rigol, and V. Galitski, *Phys. Rev. B* **84**, 241105(R) (2011).

- [38] C. Shao, E. V. Castro, S. Hu, and R. Mondaini, *Phys. Rev. B* **103**, 035125 (2021).
- [39] T. I. Vanhala, T. Siro, L. Liang, M. Troyer, A. Harju, and P. Törmä, *Phys. Rev. Lett.* **116**, 225305 (2016).
- [40] Y.-X. Wang and D.-X. Qi, *Phys. Rev. B* **99**, 075204 (2019).
- [41] I. S. Tupitsyn and N. V. Prokof'ev, *Phys. Rev. B* **99**, 121113(R) (2019).
- [42] T. Mertz, K. Zantout, and R. Valentí, *Phys. Rev. B* **100**, 125111 (2019).
- [43] B. Hetényi, *Phys. Rev. Research* **2**, 023277 (2020).
- [44] M. Z. Hasan and C. L. Kane, *Rev. Mod. Phys.* **82**, 3045 (2010).
- [45] R. R. Kumar, N. Roy, Y. R. Kartik, S. Rahul, and S. Sarkar, *arXiv: 2112.02485*.
- [46] P. Zanardi and N. Paunković, *Phys. Rev. E* **74**, 031123 (2006).
- [47] L. Campos Venuti and P. Zanardi, *Phys. Rev. Lett.* **99**, 095701 (2007).
- [48] P. Zanardi, P. Giorda, and M. Cozzini, *Phys. Rev. Lett.* **99**, 100603 (2007).
- [49] C. N. Varney, K. Sun, M. Rigol, and V. Galitski, *Phys. Rev. B* **82**, 115125 (2010).
- [50] J. Imriška, L. Wang, and M. Troyer, *Phys. Rev. B* **94**, 035109 (2016).
- [51] D. Poilblanc, *Phys. Rev. B* **44**, 9562 (1991).
- [52] Q. Niu, D. J. Thouless, and Y.-S. Wu, *Phys. Rev. B* **31**, 3372 (1985).
- [53] T. Fukui, Y. Hatsugai, and H. Suzuki, *J. Phys. Soc. Japan* **74**, 1674 (2005).
- [54] Y.-F. Zhang, Y.-Y. Y., Y. Ju, L. Sheng, R. Shen, D.-N. Sheng, and D.-Y. Xing, *Chin. Phys. B* **22**, 117312 (2013).
- [55] F. D. M. Haldane, *Phys. Rev. Lett.* **61**, 2015 (1988).
- [56] R. B. Lehoucq, D. C. Sorensen, and C. Yang, *ARPACK Users' Guide: Solution of Large Scale Eigenvalue Problems by Implicitly Restarted Arnoldi Methods* (SIAM, Philadelphia, 1997).
- [57] G. Jotzu, M. Messer, R. Desbuquois, M. Lebrat, T. Uehlinger, D. Greif, and T. Esslinger, *Nature* **515**, 237 (2014).